A Comparison of Multi-Scale 3D X-ray Tomographic Inspection Techniques for Assessing Carbon Fibre Composite Impact Damage

D.J. Bull[1*], L. Helfen[2], I. Sinclair[1], S.M. Spearing[1], T. Baumbach[2]

[1] Materials Research Group, Faculty of Engineering and the Environment, University of Southampton, Southampton, United Kingdom

[2] ANKA / Institute for Synchrotron Radiation, Karlsruhe Institute of Technology, Karlsruhe, Germany

* Corresponding author (daniel.bull@soton.ac.uk)

Keywords: A. Carbon fibres, B. Delamination, B. Impact behaviour, D. Non-destructive testing, X-ray computed tomography

Abstract

Tomographic imaging using both laboratory sources and synchrotron radiation (SR) was performed to achieve a multi-scale damage assessment of carbon fibre composites subjected to impact damage, allowing various internal damage modes to be studied in three-dimensions. The focus of this study is the comparison of different tomographic methods, identifying their capabilities and limitations, and their use in a complementary manner for creating an overall 3D damage assessment at both macroscopic and microscopic levels. Overall, microfocus laboratory computed tomography (μCT) offers efficient routine assessment of damage at mesoscopic and macroscopic levels in engineering-scale test coupons and relatively high spatial resolutions on trimmed-down samples; whilst synchrotron radiation computed tomography (SRCT) and computed laminography (SRCL) offer scans with the highest

image quality, particularly given the short acquisition times, allowing damage micromechanisms to be studied in detail.

1. Introduction

Impact damage resistance and damage tolerance have been concerns in the development of carbon fibre composite materials, particularly in aerospace structures [1]. Various damage assessment techniques have been employed to achieve a better understanding of CFRP impact damage and to develop toughening strategies [2, 3]. Ultrasonic C-scans [4] and thermography [5] are widely employed, for example; these are non-destructive testing (NDT) techniques but lack micrometer resolution and the ability to track the interaction of various damage modes within the material microstructure. Ultrasonic time of flight (TOF) scans can provide 3D representation of damage through the thickness of a laminate [6], but the nature of the scans means overlapping damage goes undetected. To achieve very high levels of detail to study the material microstructure, traditional materialographic sectioning followed by microscopy can be performed [7, 8]. However, as a destructive technique, the sample is effectively lost, risks introducing new damage during sectioning, and observed damage/displacement conditions may become non-representative due to the disturbance of residual stresses at the sectioning plane. Furthermore, physical sectioning is commonly restricted to two-dimensions (2D) on exposed surfaces; whilst this technique has been adapted to perform automated 3D analysis in the case of cross-sectional fractography [9], this is time consuming and has not been widely adopted. The focus of this paper is to examine and assess several non-destructive X-

ray tomographic techniques for the 3D examination of impact damage in composite laminates, and considers issues of resolution, sample preparation and length scales.

Considering the anisotropic properties, heterogeneous microstructure and multi-mechanistic, multi-scale nature of failure in CFRP laminates, it is relevant to take into account the 3D behaviour of the material without affecting its integrity for subsequent testing, particularly so with compression after impact (CAI) analysis. What is desirable is a technique that offers high resolution to study the internal micromechanical damage in 3D, without the issues of destroying the sample or introducing new damage. To achieve this, synchrotron radiation computed tomography (SRCT) [10-14], and in more recent work synchrotron radiation computed laminography (SRCL) [15, 16] have been successfully used to study composite materials at voxel resolutions in the order of 1 micron and below. In comparison, laboratory microfocus computed tomography (μCT) offers routine moderate resolutions, typically several micrometers and above [17-22]. These techniques have allowed key features such as micro-cracking, voids and fibre breaks within the material's structure to be assessed in considerable detail.

Recent studies have used μCT to study impact damage on composite laminate materials and have detected interlaminar and intralaminar damage within the through-thickness. In some cases contrast agents are used to detect the presence of damage [19]; this however has a limitation requiring interconnectivity between all cracks to absorb the agent which cannot be guaranteed [17]. Other studies have successfully captured 3D damage without the use of contrast agents [23-25]. A major

challenge in standard μCT imaging using a large-area (e.g. flat panel) detector is that for reaching high spatial resolutions (e.g. 10 μm and less), flat specimens cannot be fully turned due to collision with the X-ray tube housing which effectively limits the angular acquisition range. In most studies the specimens are hence cut to smaller sample sizes. To our knowledge, no work using SRCT or SRCL to study composite impact damage has been published so far.

SRCL, SRCT and μCT operate on similar principles: a large number of 2D radiographic projections are taken as the sample in question is rotated. These radiographs undergo an inverse Radon Transform via a variety of possible methods to form a 3D volume. The two key differences between these techniques are the X-ray sources - use of synchrotron vs. micro-focus tube - and the axis of rotation for scan acquisition; this is perpendicular to the X-ray beam in computed tomography (CT), and tilted to less than 90˚ in computed laminography (CL). Key benefits of synchrotron imaging include fast acquisition speed with high signal-to-noise, convenient exploitation of phase contrast effects particularly propagation methods for enhanced edge detection [26], and sub-micrometer resolutions, when compared to conventional micro-focus sources [27].

With respect to the axis of rotation in scanning, a significant drawback of CT is that it is best suited to samples with relatively isotropic cross-section shapes, for example circular or square, in cases for which the highest resolutions, signal-to-noise and artefact avoidance are required [15]. The laterally extended geometry of typical engineering-level impact coupons therefore requires regions of interest (ROIs) to be physically cut from the specimen to conform to these geometries. Whilst this can work

well [17, 19] it clearly obviates the non-destructive character of whole-object CT. CL presents one solution to this limitation in CT for flat objects in its simplest and basic form by maintaining reasonably uniform X-ray transmission at all angles, allowing non-destructive 3D inspection of ROIs within almost arbitrarily extended planar samples at micrometer and sub-micrometer resolutions [28, 29]. In various fields of materials science, these resolution ranges render the method particularly adapted to study microstructures [30, 31] and their temporal evolution under different loading conditions [32-34].

The present paper specifically explores the use of SRCT, SRCL and µCT on relatively thin (1 mm) impacted coupons of CFRP laminate, to evaluate their uses in a complementary manner. The feasibility of using high resolution SRCL is reported for thicker (4.5 mm) samples conforming to the ASTM D7136M [35] impact standard in addition to local low resolution µCT of complete intact plates. This work differs from previous work by forming a direct comparison of 3D imaging methods on impacted CFRP panels.

2. Materials and Methods

2.1 Material

Cytec prototype unidirectional CFRP prepreg material with a layup of $[+45/0/-45/90]_s$ was cut to form 80 x 80 mm coupons with a thickness of 1 mm. The thicker 4.5 mm specimens had a layup of $[+45/0/-45/90]_{3s}$, these were cut to 150 x 100 mm. Particle toughened resin systems were used in this study. The coupons were ultrasonically C-scanned to check for gross manufacturing defects on the mm scale prior to impact.

2.2 Mechanical testing

Impact testing was achieved via a drop tower system to ASTM D7136 standards [35] with a striker mass of 4.9 kg and a hemispherical 16 mm diameter tup. The specimens were impacted at 1.3 J and 30 J for the 1 mm and 4.5 mm thick specimens respectively. In order to accommodate 1 mm thick specimens, a non-standard base plate was used consisting of a circular 60 mm diameter window supported by a ring of the same dimensions as used in [36]. The 4.5 mm samples were supported over a 125x75 mm base plate using four toggle clamps. After impact, specimens were C-scanned to measure the overall extent of the impact damage area. Again, the resolution of the C-scan was approximately 1 mm.

2.3 Imaging sample preparation

CT studies were performed on ROIs cut from the panel. For the 1 mm laminate, a low speed diamond cutting wheel was used to cut 4.5 x 80 x 1 mm 'matchsticks' across the damaged impact site as determined from ultrasonic C-scans. The corresponding 'matchsticks' were then stacked in pairs to form 4.5 x 80 x 2 mm specimens to be scanned together in one operation. No specific material preparation was required for samples used in SRCL imaging; regions within the damage area were targeted.

For the 4.5mm laminate, ROIs were physically cut to 4.5 x 4.5 x 150 mm 'matchstick' for µCT analysis, having already been SRCL scanned in the complete condition. To test the feasibility of locally scanning intact plates using µCT, plates were stacked and scanned in pairs. This was to reduce the width to thickness aspect ratio thus reducing variations in X-ray path length and to fully fill the available field of view in the volume

allowing two samples to be scanned at once. The intact plate was scanned at the maximum voxel resolution determined by the clearance between the target and the object to allow a full rotation.

2.4 X-ray tomography

Settings used for µCT, SRCT and SRCL scanning are summarised in Table 1. Two settings were used on the µCT scanner for 'matchstick' specimens and intact 4.5 mm thick plates. Scans were reconstructed via filtered back projection methods in all cases. µCT scans were undertaken at the University of Southampton µ-VIS Centre on a Nikon Metrology HMX 225 CT system, using a molybdenum target without filtration.

SRCT and SRCL scans were carried out at the European Synchrotron Radiation Facility (ESRF) on beamline ID19, providing an intense, parallel, essentially monochromatic and coherent beam that supports simple propagation-based and phase-enhanced contrast, free of beam hardening and cone geometry artefacts when compared to cone beam micro-focus CT [27, 37]. To achieve high resolution, the projection images for both SRCT and SRCL were captured via a thin-film scintillator and optical microscope imaging system, consistent with the non-divergent parallel beam. The cone beam geometry of the µCT provides geometric magnification, with images being captured on a large CMOS flat panel (Perkin-Elmer 1621 model).

SRCT and SRCL scan geometries are illustrated schematically in Fig. 1(a) and (b), with the rotational axis inclined at an angle to the incident beam in the case of CL [38], rather than perpendicular in standard CT. As such, CL is substantially better suited for high resolution scanning of laterally extended objects by minimising two issues

highlighted in Fig. 1(a): firstly, the large variations in X-ray path length which occur as the object is rotated; secondly, the movement-into-view of material not intended as part of the scanned volume, and the inclusion of this in the projections. In cases where the geometry of the plate leads to a significant angular range of missing projections due to absorption along the longest path in CT scans, it has been reported that CL performs better than CT as discussed in [39].

Whilst the viability of strategies for local ROI imaging in CT is demonstrated in this paper, compromises remain in balancing signal-to-noise ratio and artefacts - such as streaking, ring artefacts and beam hardening - in the imaging and reconstruction process [28, 40]. From the perspective of the Central Slice Theorem, CL represents incomplete sampling of the 3D Fourier domain during scanning, also resulting in reconstruction artefacts, which may be minimised to some extent via the reconstruction process [15, 38].

3. Results and discussion

3.1 Initial observations

All three techniques yield reasonably clear imaging of overall larger-scale damage modes associated with impact loading, particularly interlaminar and intralaminar cracking: a cross-sectional slice of the reconstructed volumes shows representative image qualities in Fig. 2(a-c) for µCT, SRCT and SRCL respectively. All results are shown in a mostly unprocessed state, i.e. no image-domain filtering or enhancements are applied. For direct comparison, Fig. 2 (a and b) show the same location within the same sample, and (c) is of a different sample at a similar damage region. Whilst both

CT techniques involved specimen cutting, comparing this data to the non-destructive SRCL technique shows qualitatively comparable levels of damage visualisation, with similar damage morphologies and apparent crack opening displacements (COD). There was limited evidence of additional damage being introduced to the CT specimen volumes during cutting, although it is possible that some surface damage is introduced, particularly where sectioning across areas that are severely damaged during impact.

Although individual fibres could not be detected in the μCT scans at the moderate voxel resolution selected here, individual plies and their interfaces could be distinguished as well as the presence of cracks, including those with CODs less than the voxel size used in the scan. The two SR methods shown in Fig. 2(b) and (c) demonstrate the benefits of phase-enhanced edge contrast and increased resolution: details of individual fibres and resin rich regions are clearly visible, with damage micromechanisms clearly delineated. SRCT and SRCL yield qualitatively similar damage visualisation employing the edge-enhancing phase contrast [26, 28], with the benefit of SRCL being the intact coupon geometry. However in the case of SRCL, artefacts resulting from incomplete Fourier-space sampling can arise: an exact inversion of the modulation transfer function (MTF) is not possible. Using a filtering step for the 2D projection prior to backprojection data minimises artefacts in the 3D reconstructed volume [28, 38]. Additional artefacts appearing in this study were particularly evident at the edges of the volume in places where not all projections contribute to the reconstructed image. Additional artefacts in the reconstructed 3D images of SRCL will have direct implications for automated segmentation and feature extraction processes, inevitably increasing the complexity of such processes.

Delaminations are a key damage mode in impact loading, in which micro-scale data for the crack morphology and shear and opening displacements is important [41, 42]. A comparison of the same delamination shown in Fig. 3(a/b) obtained using µCT and SRCT techniques respectively, and a similar delamination obtained with SRCL in Fig. 3(c) highlights the role of multi-scale imaging. Assessment of the delamination via µCT at moderate resolution suggests the presence of a continuous crack with a single bridged section. The greater level of detail obtained from both SR techniques shows that the micromechanisms are more complicated, with significant incidence of fine-scale crack bridging within the resin rich regions.

3.2 Sub-voxel assessment of µCT data

It is reported that sub-voxel data may be captured from CT data [43], as illustrated in Fig. 4(a i-ii). Direct comparison with the SRCT data for the low resolution µCT data indicated that cracks with an opening displacement as low as 30% of the voxel resolution were reliably captured with µCT, in keeping with previous comparisons between µCT and conventional microscopy [11, 17]. Fig. 5 illustrates the significance of partial volume effect on crack detection via grey-scale plots across the crack openings indicated by the lines in Fig. 4(a i-iv). The presence of a crack is indicated by a minimum on the line plot and, in the case of sub-voxel data, this minimum falls between the bounds of the mean grey-scale values of air and material. In the presence of complex crack bridging ligaments, it is clear that whilst the CODs from these cracks cannot be measured via µCT to high accuracy for example by exploiting weighted averages of bulk greyscale values to deduce partial volume effects [43], they show the locations and extent of damage. This informs the general mechanics of

failure, in addition to identifying ROIs for more detailed analysis. It may be noted that to achieve greater effective contrast in crack detection penetrant dyes may be employed [17, 19, 20]; however impact damage analysis presents limited scope for penetrant use given the presence of many non-surface breaking cracks, particularly in the critical Barely Visible Impact Damage (BVID) regime.

3.3 3D segmentation

The 3D morphology of impact damage was segmented via the semi-automatic 'seed growth' approach [44] in the same 'matchstick' specimen using µCT and SRCT data, as shown in Fig. 6(a/b). The field of view for SRCT was smaller than that of µCT, hence the smaller segmented volume. µCT and SRCT both give a reasonable mechanistic representation of 3D damage, nonetheless the reduced resolution of µCT means that even though sub-voxel information can be extracted to some extent, information is lost when crack opening displacements (COD) start approaching the lower limits of detection.

A compromise between resolution and the overall size of the volume needs to be met. At the 4.3 micrometer voxel resolution used in this study, µCT gives damage representation over a sample volume cross-section of approximately 1 cm. Additionally measurements of crack lengths can be approximated, although information towards the tips of the crack will be missed where crack openings are down to 30% of the voxel resolution, leading to an underestimation of the crack length. To achieve the microscopic detail required to capture the undetected or non-segmentable damage, SR techniques are clearly of significant value (e.g. in identifying

the role of traction forces due to ligament formation across cracks) at the expense of reduced overall fields of view. Multiple scans may of course be taken to capture a larger proportion of damage; however increased computational costs in terms of data size and post-processing load are non-trivial.

3.4 SRCL: analysis of thick specimen

Whilst the above results are based on 1 mm thick laminate samples, to study impact damage within a conventional engineering context it is desirable to achieve high resolution non-destructive scans of specimens meeting standard impact test conditions such as ASTM D7136. For a D7136 compliant coupon thickness of 4.5 mm, the SRCL conditions noted above led to a scanning condition that is local in terms of both in-plane position, and through-thickness position. As such, by adjusting the location of the specimen so that the ROI lies at the point where the tilted centre of rotation intercepts the beam, localised volumes through the thickness of the material may be generated within the specimen.

Fig. 7(a) illustrates such a typical 'local' SRCL result for a 4.5 mm thick CFRP plate, demonstrating that high resolution imaging is indeed possible for such a full-thickness intact impact coupon. Artefacts consisting of vertical streaks are present towards the image corners as indicated by arrows, as these regions are increasingly out of view across the full scan rotation. These artefacts occur at similar image locations with the 1mm specimens shown in Fig. 2(c).

A direct comparison of this local SRCL region Fig. 7(a) is compared with a µCT 'matchstick' scan of the same region shown in (b) with the corresponding SRCL

location indicated by the box. The overall image quality from SRCL is sufficient to identify individual fibres, cracking and small voids, with the latter two features also being detected with µCT. Limited contrast is particularly noticeable for the large continuous delamination crack seen in the upper half of Fig. 7(a) and the corresponding boxed area of Fig. 7(b), consistent with this crack lying in a plane which is not directly sampled by the tilted rotation axis used for CL, highlighting the direction dependence of image quality in a limited angular access geometry such as CL. Reasonably similar image qualities in detecting intralaminar cracking in 4.5 mm and 1 mm thick sample are illustrated in Fig. 8, consistent with the modest absorption of CFRP for these thicknesses at the associated X-ray energy level.

Considering that SRCL allows for truly non-destructive, high resolution testing on ASTM standard panels, one may identify SRCL as a preferred analysis method for materials performance analysis under standard impact conditions. However high resolution SRCL carried out over the large areas that may be associated with an impact event clearly carries a potentially high synchrotron beamtime and computational/data handling load.

3.5 µCT: local scan on intact thick specimen

Whilst SRCL offers non-destructive assessment of full ASTM standard panels, time and beam access constraints apply. As an alternative, µCT scans of complete intact panels are also of interest and offer rapid global assessment at intermediate voxel resolutions, as obtained in [22] and [25]. The voxel resolution was limited by how close the specimen could be positioned to the X-ray target source. Local scans of full plates

were tested using µCT and importantly this was achieved using relatively fast micro-focus CT settings. A cross-sectional slice of such a scan is shown in Fig. 9. Despite the non-ideal geometry of the sample for CT assessment compared to the near 'matchstick' samples and the lower 14.3 µm voxel resolution used, primary damage mechanisms were clearly detected. Whilst limited in resolution, the ability to image meso- to macro-scale damage characteristics in the absence of synchrotron access remains a valuable complementary approach. In particular, extended time-resolved studies of damage propagation under incrementally increasing compressive loads, where truly global assessment across a complete damage zone in the order of centimetres in diameter via SRCL would be excessive in both beamtime and the amount of data generated.

4. Conclusions

It is evident that for the mixed length scales associated with impact events, different X-ray imaging methods offer alternative and complementary combinations of image resolution and fidelity, sample preparation requirements, limitations and hardware availability.

At routinely achievable voxel resolutions laboratory µCT offers valuable detail for understanding the three-dimensional macro and mesoscopic extent of impact damage, with reliable sub-voxel detection of the extent of cracks being illustrated. SR techniques (SRCT and SRCL) allow for rapid scanning of 3D micro-scale damage down to the scale of individual fibres. Laboratory µCT systems alternatively offer scan volumes up to tens of cm, capturing entire impact sites in a single scan on complete

panels. This coupled with a fast scan setting make it feasible to perform *ex situ* time series work enabling 3D damage propagation to be monitored.

Comparing the damage morphologies of the 3D segmentation of the same sample obtained using µCT and SRCT, both techniques show similar results for capturing the overall extent of damage. However, where greater mechanistic detail is required, SR techniques are clearly superior, particularly in terms of the speed at which low noise, high resolution scans may be obtained.

The potential for local, very high resolution 3D analysis of complete, engineering-scale impact test panels is demonstrated for synchrotron laminography, offering unique opportunities for 'through-process' assessment of compression after impact analysis; i.e. intact impacted panels being examined non-destructively at high resolution, prior to compression testing. However, integration within a program of more conventional and accessible testing and imaging modalities is likely to be required for effective use of such limited, specialised capabilities.

5. Acknowledgements

Thanks to the ESRF for use of their SRCT and SRCL facilities on beamline ID19. Additional thanks go to µ-VIS at the University of Southampton for their µCT and computer analysis facilities and the EPSRC for their funding of the project. The paper acknowledges Cytec for their sponsorship and supply of materials used in this project with appreciation to Sam Hill and Dr Kingley Kin Chee Ho, for their input as the technical point of contact.

References

[1] Soutis C. Carbon fiber reinforced plastics in aircraft construction. Mat Sci Eng a-Struct. 2005;412(1-2):171-176.
[2] Gao SL, Kim JK. Three-dimensional characterization of impact damage in CFRPs. Key Eng Mat. 1998;141-1:35-53.
[3] Greenhalgh ES. Failure analysis and fractography of polymer composites. Oxford: Woodhead Publishing Ltd.; 2009.
[4] Aymerich F, Meili S. Ultrasonic evaluation of matrix damage in impacted composite laminates. Compos Part B-Eng. 2000;31(1):1-6.
[5] Vavilov V, Marinetti S, Grinzato E, Bison PG. Thermal tomography, characterization and pulse phase thermography of impact damage in CFRP, or why end-users are still reluctant about practical use of transient IR thermography. Thermosense Xx. 1998;3361:275-281.
[6] de Freitas M, Silva A, Reis L. Numerical evaluation of failure mechanisms on composite specimens subjected to impact loading. Compos Part B-Eng. 2000;31(3):199-207.
[7] Rio TGD, Zaera R, Barbero E, Navarro C. Damage in CFRPs due to low velocity impact at low temperature. Compos Part B-Eng. 2005;36(1):41-50.
[8] Shyr TW, Pan YH. Impact resistance and damage characteristics of composite laminates. Compos Struct. 2003;62(2):193-203.
[9] Boll DJ, Bascom WD, Weidner JC, Murri WJ. A Microscopy Study of Impact Damage of Epoxy-Matrix Carbon-Fiber Composites. J Mater Sci. 1986;21(8):2667-2677.
[10] Moffat AJ, Wright P, Buffiere JY, Sinclair I, Spearing SM. Micromechanisms of damage in 0 degrees splits in a [90/0](s) composite material using synchrotron radiation computed tomography. Scripta Mater. 2008;59(10):1043-1046.
[11] Wright P, Moffat A, Sinclair I, Spearing SM. High resolution tomographic imaging and modelling of notch tip damage in a laminated composite. Compos Sci Technol. 2010;70(10):1444-1452.
[12] Wright P, Fu X, Sinclair I, Spearing SM. Ultra high resolution computed tomography of damage in notched carbon fiber-epoxy composites. J Compos Mater. 2008;42(19):1993-2002.
[13] Aroush DRB, Maire E, Gauthier C, Youssef S, Cloetens P, Wagner HD. A study of fracture of unidirectional composites using in situ high-resolution synchrotron X-ray microtomography. Compos Sci Technol. 2006;66(10):1348-1353.
[14] Scott AE, Mavrogordato M, Wright P, Sinclair I, Spearing SM. In situ Fibre Fracture Measurement in Carbon-Epoxy Laminates using High Resolution Computed Tomography. Compos Sci Technol.In Press, Accepted Manuscript.
[15] Moffat AJ, Wright P, Helfen L, Baumbach T, Johnson G, Spearing SM, et al. In situ synchrotron computed laminography of damage in carbon fibre-epoxy [90/0](s) laminates. Scripta Mater. 2010;62(2):97-100.
[16] Xu F, Helfen L, Moffat AJ, Johnson G, Sinclair I, Baumbach T. Synchrotron radiation computed laminography for polymer composite failure studies. J Synchrotron Radiat. 2010;17:222-226.
[17] Schilling PJ, Karedla BPR, Tatiparthi AK, Verges MA, Herrington PD. X-ray computed microtomography of internal damage in fiber reinforced polymer matrix composites. Compos Sci Technol. 2005;65(14):2071-2078.
[18] Sugimoto S, Aoki T, Iwahori Y, Ishikawa T. Nondestructive evaluation of composites using Micro-Focused X-Ray CT Scanner. Aip Conf Proc. 2005;760:1081-1086.
[19] Tan KT, Watanabe N, Iwahori Y. X-ray radiography and micro-computed tomography examination of damage characteristics in stitched composites subjected to impact loading. Compos Part B-Eng. 2011;42(4):874-884.

[20] Bathias C, Cagnasso A. Application of X-Ray Tomography to the Nondestructive Testing of High-Performance Polymer Composites. Am Soc Test Mater. 1992;1128:35-54.
[21] Pandita SD, Falconet D, Verpoest I. Impact properties of weft knitted fabric reinforced composites. Compos Sci Technol. 2002;62(7-8):1113-1123.
[22] Enfedaque A, Molina-Aldareguia JM, Galvez F, Gonzalez C, Llorca J. Effect of Glass Fiber Hybridization on the Behavior Under Impact of Woven Carbon Fiber/Epoxy Laminates. J Compos Mater. 2010;44(25):3051-3068.
[23] Archer E, King, S, Quinn, JP, Buchanan, S and McIlhagger. Impact damage analysis of 3D woven carbon fibre composites using computed tomography. 18th international conference on composite materials, vol. W02 South Korea: The Korean society for composite materials; 2011. p. 6.
[24] Crupi V, Epasto G, Guglielmino E. Computed Tomography analysis of damage in composites subjected to impact loading. V Crupi et alii, Frattura ed Integrità Strutturale. 2011;17:32-41.
[25] McCombe GP, Rouse J, Trask RS, Withers PJ, Bond IP. X-ray damage characterisation in self-healing fibre reinforced polymers. Compos Part a-Appl S. 2012;43(4):613-620.
[26] Cloetens P, PateyronSalome M, Buffiere JY, Peix G, Baruchel J, Peyrin F, et al. Observation of microstructure and damage in materials by phase sensitive radiography and tomography. J Appl Phys. 1997;81(9):5878-5886.
[27] Baruchel J, Buffiere JY, Cloetens P, Di Michiel M, Ferrie E, Ludwig W, et al. Advances in synchrotron radiation microtomography. Scripta Mater. 2006;55(1):41-46.
[28] Helfen L, Myagotin A, Rack A, Pernot P, Mikulik P, Di Michiel M, et al. Synchrotron-radiation computed laminography for high-resolution three-dimensional imaging of flat devices. Phys Status Solidi A. 2007;204(8):2760-2765.
[29] Xu F, Helfen L, Suhonen H, Elgrabli D, Bayat S, Reichig P, et al. 3D imaging of structure and composition in extended objects. manuscript accepted for publication. in press 2012.
[30] Maurel V, Helfen L, N'Guyen F, Koster A, Di Michiel M, Baumbach T, et al. Three-dimensional investigation of thermal barrier coatings by synchrotron-radiation computed laminography. Scripta Mater. 2012;66(7):471-474.
[31] Helfen L, Morgeneyer TF, Xu F, Mavrogordato MN, Sinclair I, Schillinger B, et al. Synchrotron and neutron laminography for three-dimensional imaging of devices and flat material specimens. Int J Mater Res. 2012;103(2):170-173.
[32] Morgeneyer TF, Helfen L, Sinclair I, Proudhon H, Xu F, Baumbach T. Ductile crack initiation and propagation assessed via in situ synchrotron radiation-computed laminography. Scripta Mater. 2011;65(11):1010-1013.
[33] Tian T, Xu F, Han JK, Choi DC, Cheng Y, Helfen L, et al. Rapid diagnosis of electromigration induced failure time of Pb-free flip chip solder joints by high resolution synchrotron radiation laminography. Appl Phys Lett. 2011;99(8).
[34] Morgeneyer TF, Helfen L, Mubarak H, Hild F. 3D digital volume correlation of synchrotron radiation laminography images of ductile crack initiation: an initial feasibility study. Exp Mech. in press 2012.
[35] ASTM D 7136/D 7136M 07 Standard Test Method for Measuring the Damage Resistance of a Fiber-Reinforced Polymer Matrix Composite to a Drop-Weight Impact Event. ASTM International; 2007.
[36] Sanchu-Saez S, Barbero E, Zaera R, Navarro C. Compression after impact of thin composite laminates. Compos Sci Technol. 2005;65(13):1911-1919.
[37] Salvo L, Cloetens P, Maire E, Zabler S, Blandin JJ, Buffiere JY, et al. X-ray micro-tomography an attractive characterisation technique in materials science. Nucl Instrum Meth B. 2003;200:273-286.

[38] Helfen L, Baumbach T, Mikulik P, Kiel D, Pernot P, Cloetens P, et al. High-resolution three-dimensional imaging of flat objects by synchrotron-radiation computed laminography. Appl Phys Lett. 2005;86(7):071915.
[39] Xu F, Helfen L, Baumbach T, Suhonen H. Comparison of image quality in computed laminography and tomography. Opt Express. 2012;20(2):794-806.
[40] Barrett JF, Keat N. Artifacts in CT: Recognition and Avoidance. Radiographics. 2004;24(6):1679-1691.
[41] Greenhalgh E, Hiley M. The assessment of novel materials and processes for the impact tolerant design of stiffened composite aerospace structures. Compos Part a-Appl S. 2003;34(2):151-161.
[42] Takeda N, Sierakowski RL, Malvern LE. Microscopic observations of cross sections of impacted composite laminates Composites Technology Review. 1982;4(2):40-44.
[43] Guvenilir A, Breunig TM, Kinney JH, Stock SR. New direct observations of crack closure processes in Al-Li 2090 T8E41. Philos T Roy Soc A. 1999;357(1761):2755-2775.
[44] Scott AE, Mavrogordato M, Wright P, Sinclair I, Spearing SM. In situ fibre fracture measurement in carbon-epoxy laminates using high resolution computed tomography. Compos Sci Technol. 2011;71(12):1471-1477.

Table 1 - µCT, SRCT and STCL imaging conditions

	µCT (matchsticks)	µCT (Intact plate)	SRCT	SRCL
Energy (kV)	65 (peak) ~24 (mean)	115 (peak) ~40 (mean)	19 (monochromatic)	19 (monochromatic)
Gun current (µA)	70	100	-	-
Voxel resolution (μm^3)	4.3	14.2	1.4	0.7
Number of radiographs	2000 (360˚)	1301	1500 (180˚)	1500 (360˚)
Exposure time (ms)	2,000	1,000	100	100
Total scan time (min)	150	44	5	11

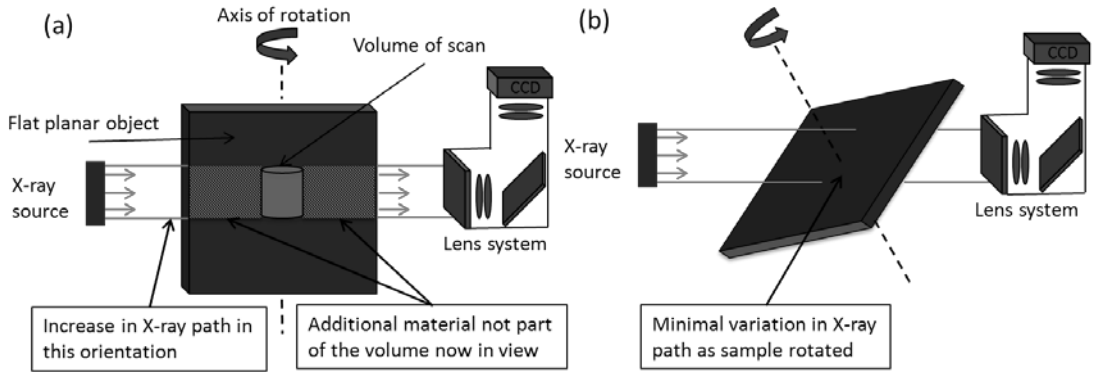

Fig. 1 Schematic of high resolution scanning techniques for extended planer objects: (a) SRCT and (b) SRCL.

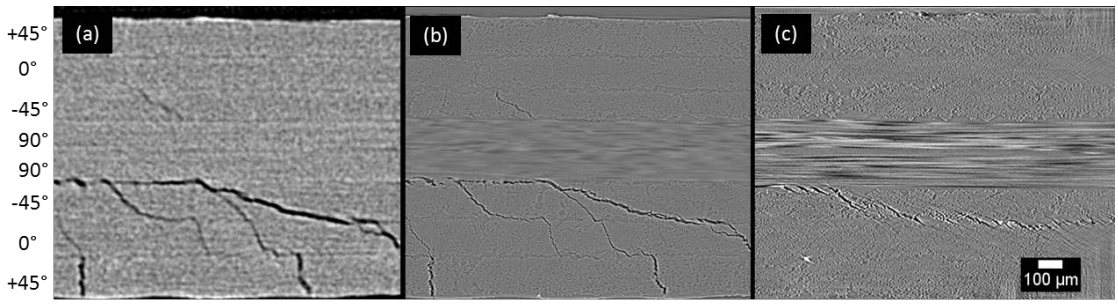

Fig. 2 Cross-sectional views of impact damage via: (a) µCT, (b) SRCT and (c) SRCL. Images (a) and (b) are of the same sample at the same location, whilst (c) is of a similar damage region of a different sample.

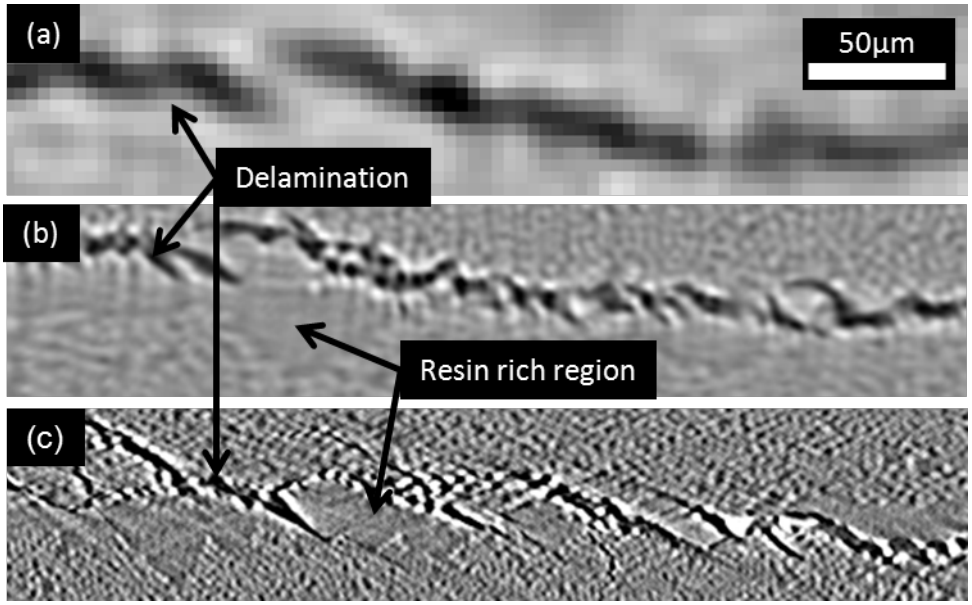

Fig. 3 Close up of a delaminated region obtained using (a) µCT (b) SRCT (c) and SRCL. (a) and (b) are of the same specimen at approximately the same location, (c) is representative of similar damage on a separate specimen.

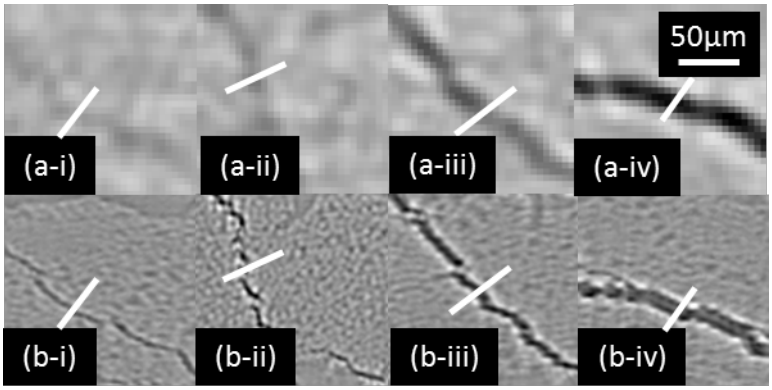

Fig. 4 Cracks of varying COD level (approximate) (i-iv) <1.4, 3, 4, and 8 µm respectively, comparisons of image quality between (a) µCT and (b) SRCT.

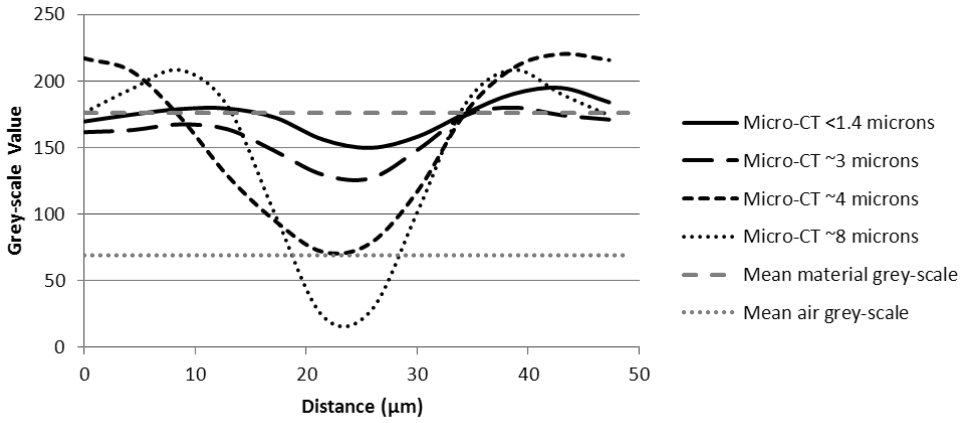

Fig. 5 Line-plot showing the corresponding µCT grey-scale values across the opening of cracks ranging from crack opening displacements of <1.4 to ~8 micrometers.

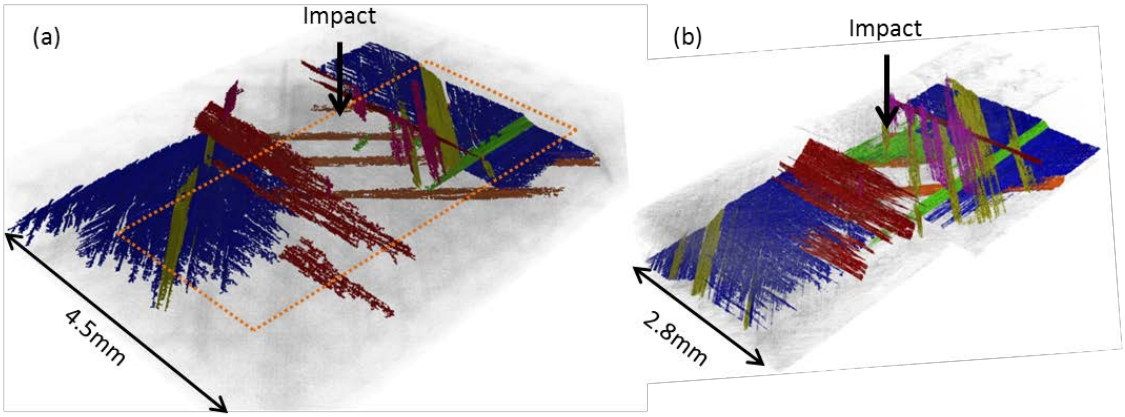

Fig. 6 3D segmentation revealing the damage morphology surrounding the impact region within the same specimen obtained by (a) µCT with the dotted region indicating the region obtained using (b) SRCT. Blue is representative of delaminations whilst other colours indicate matrix cracking occurring on each respective ply.

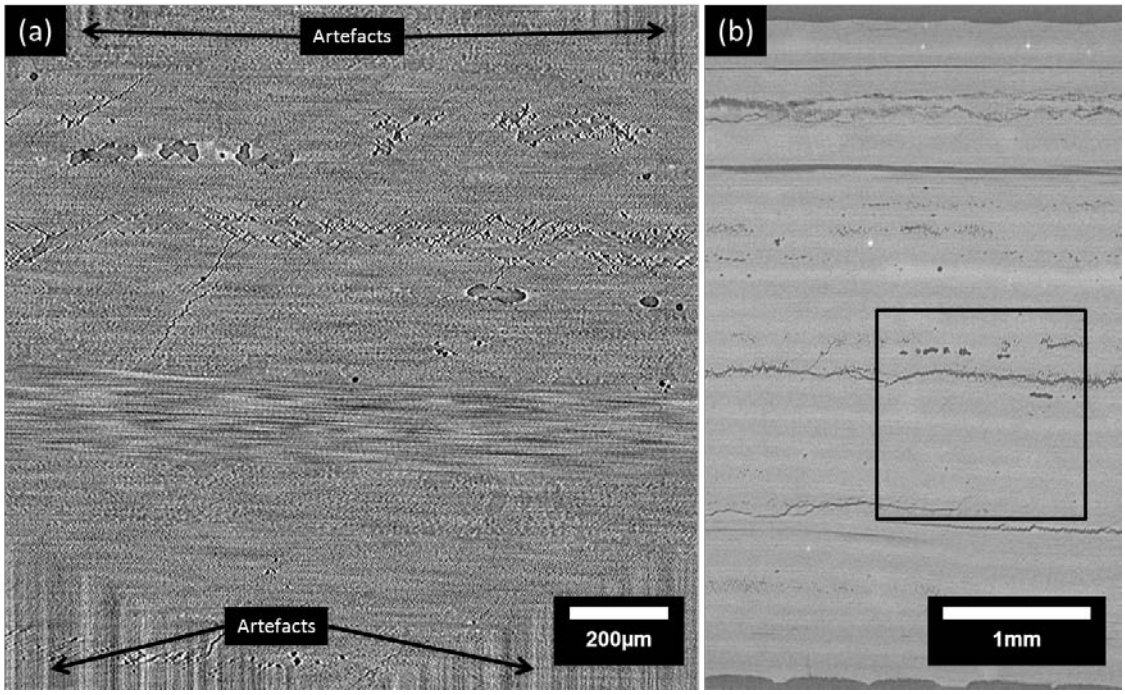

Fig. 7 Cross-sectional view of an impacted 4.5mm thick specimen, (a) mid-way through the cross-sectional thickness obtained using SRCL and (b) corresponding μCT slice, with box showing the location of the SRCL scan within the through thickness.

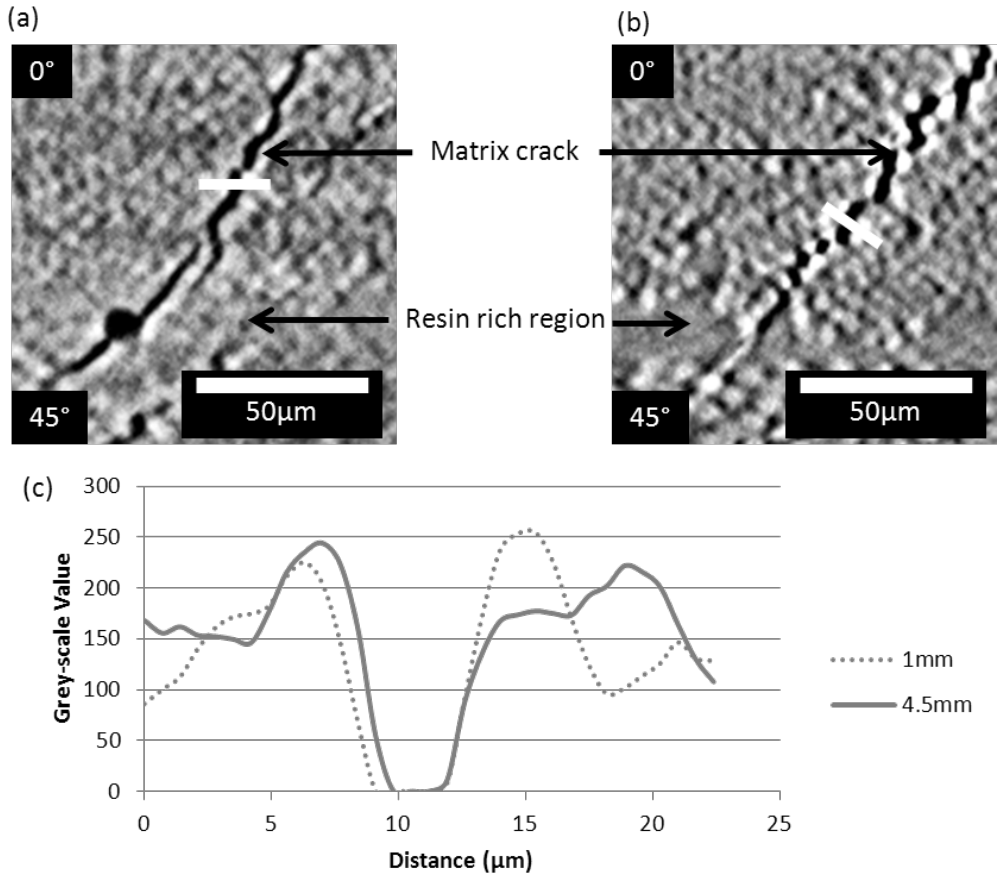

Fig. 8 Close up of a crack obtained using SRCL of 4.5mm thick specimen (a) and 1mm specimen (b), the white lines indicate a region across the crack to obtain the line plots shown in (c).

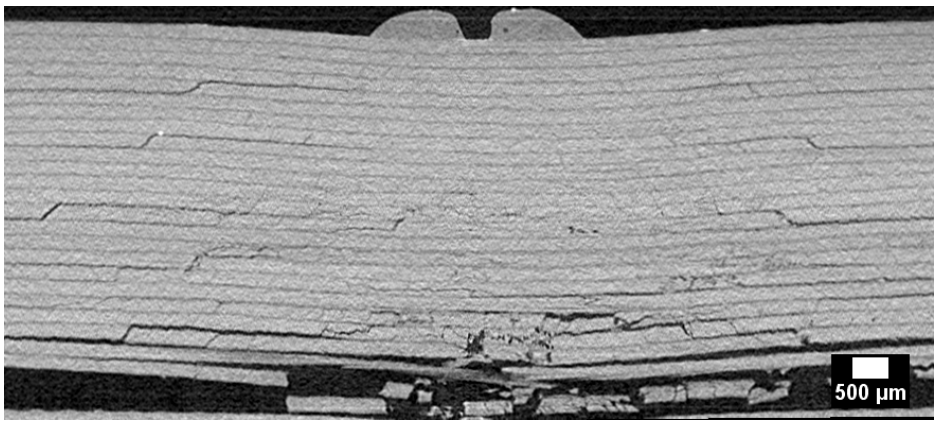

Fig. 9 Cross-section of a ~4.5mm thick CFRP laminate sample obtained by a local µCT scan of an intact panel.